# The uvsY Recombination Protein of Bacteriophage T4 Forms Hexamers in the Presence and Absence of Single-Stranded DNA†

Hans T. H. Beernink and Scott W. Morrical*

*Department of Biochemistry, Department of Microbiology and Molecular Genetics, and Vermont Cancer Center, University of Vermont College of Medicine, Burlington, Vermont 05405*

*Received January 13, 1998; Revised Manuscript Received March 3, 1998*

ABSTRACT: A prerequisite to genetic recombination in the T4 bacteriophage is the formation of the presynaptic filament—a helical nucleoprotein filament containing stoichiometric amounts of the uvsX recombinase in complex with single-stranded DNA (ssDNA). Once formed, the filament is competent to catalyze homologous pairing and DNA strand exchange reactions. An important component in the formation of the presynaptic filament is the uvsY protein, which is required for optimal uvsX−ssDNA assembly in vitro, and essential for phage recombination in vivo. uvsY enhances uvsX activities by promoting filament formation and stabilizing filaments under conditions of low uvsX, high salt, and/or high gp32 (ssDNA-binding protein) concentrations. The molecular properties of uvsY include noncooperative binding to ssDNA and specific protein−protein interactions with both uvsX and gp32. Evidence suggests that all of these hetero-associations of the uvsY protein are important for presynaptic filament formation. However, there is currently no structural information available on the uvsY protein itself. In this study, we present the first characterization of the self-association of uvsY. Using hydrodynamic methods, we demonstrate that uvsY associates into a stable hexamer ($s^0_{20,w} = 6.0$, $M = 95$ kDa) in solution and that this structure is competent to bind ssDNA. We further demonstrate that uvsY hexamers are capable of reversible association into higher aggregates in a manner dependent on both salt and protein concentration. The implications for presynaptic filament formation are discussed.

The uvsY protein is an essential component of the general recombination machinery of bacteriophage T4. The 15.8 kDa uvsY protein lacks enzymatic activities of its own, yet serves as an accessory protein to the T4 general recombinase, uvsX protein, modulating virtually all reactions catalyzed by the latter enzyme (*1*−*4*). In vitro, uvsY stimulates the ssDNA[1]-dependent ATPase activity of uvsX protein, lowers the critical concentrations of uvsX protein required for DNA strand exchange and recombination-dependent DNA synthesis reactions, and overcomes the inhibition of uvsX-catalyzed reactions caused by low uvsX and/or high salt concentrations, and by high concentrations of gp32, the T4-encoded ssDNA-binding protein (*1*−*6*). These stimulatory effects of uvsY on uvsX appear to be essential for recombination in vivo, since the recombination-deficiency phenotypes of T4 *uvsY*$^-$ and *uvsX*$^-$ single mutants are generally indistinguishable (*7*−*10*). In addition to reduced recombination frequencies, these phenotypes include DNA arrest and UV sensitivity, corresponding to the roles of T4 recombination machinery in initiating phage DNA replication and in recombinational DNA repair (*8*, *10*; reviewed in *11*).

uvsY appears to exert its major effect on uvsX recombination functions by nucleating the assembly of, and then stabilizing, uvsX−ssDNA presynaptic filaments (*1*, *2*, *4*). To understand the mechanism of uvsY action in promoting presynapsis, it is necessary to understand the biochemical properties of uvsY protein, which include noncooperative, non-sequence-specific binding to ssDNA (*12*), and specific protein−protein interactions with both the uvsX and gp32 proteins (*13*−*15*). Evidence suggests that all three of these hetero-associations of uvsY protein are important for its function (*2*, *15*, *16*). The interactions of uvsY with ssDNA and gp32 may function to allow the binding of uvsY to gp32-coated ssDNA, leading to the recruitment of uvsX and nucleation of filaments (*15*; unpublished experiments). At the same time, uvsY−uvsX interactions appear to be important for stabilizing uvsX−ssDNA filaments (*2*). However, the precise biochemical mechanisms by which uvsY performs both its nucleation and stabilization functions remain to be elucidated.

An important unanswered question regarding the uvsY protein is its oligomeric structure. Both uvsX protein and gp32 bind cooperatively to ssDNA (*17*−*19*), and their self-association properties are of obvious importance to the recombination system. Rigorous characterization of uvsY−ssDNA interactions demonstrated that this protein clearly binds noncooperatively to ssDNA (*12*); nevertheless, uvsY−uvsY cross-linking is observed under some conditions in

† This work was supported by NIH Research Grant GM48847 (to S.W.M.) and by NCRR−BRS Shared Instrumentation Grant RR11293. H.T.H.B. was supported in part by Training Grant ES07122 from the NIEHS.

* To whom correspondence and reprint requests should be addressed. Telephone: 802-656-8260. FAX: 802-862-8229. E-mail: smorrica@zoo.uvm.edu.

[1] Abbreviations: ssDNA, single-stranded DNA; ϵDNA, etheno-modified ssDNA; gp32, T4 gene 32 protein; KOAc, potassium acetate; Gua-HCl, guanidine hydrochloride; HPLC, high-performance liquid chromatography; oligo($dT_{25}$), 25-mer homo-oligonucleotide dT.

S0006-2960(98)00095-6 CCC: $15.00 
Published on Web 04/02/1998

vitro, in both the presence and absence of ssDNA (*15*, *20*). Thus, it appears likely that uvsY interacts with ssDNA (and perhaps with protein components of the system as well) in greater than monomeric form, which could be extremely important for its function in recombination. Accordingly, here we present the first physical characterization of the self-association properties of the T4 uvsY protein. Using hydrodynamic methods including sedimentation velocity, sedimentation equilibrium, and size exclusion chromatography, we demonstrate: (1) that uvsY protein exists as a stable hexamer in solution under conditions of moderate to high salt concentrations; (2) that uvsY hexamers undergo further, reversible self-association to higher forms in a salt- and concentration-dependent manner; and (3) that the uvsY hexamer binds to ssDNA as an intact unit, with subtle changes in hydrodynamic behavior that may reflect conformational alterations in the uvsY−ssDNA complex. We relate these findings to previous studies of uvsY−ssDNA interactions and to possible models for presynapsis in the T4 recombination system.

## EXPERIMENTAL PROCEDURES

*Reagents and Buffers.* All buffers and solutions were made using reagent-grade chemicals and deionized, glass-distilled water. All chemicals and biochemicals were purchased from Sigma unless otherwise noted. Analytical Ultracentrifugation (AnU) buffers contained 20 mM Tris-HCl, pH 7.4, 1 mM $MgCl_2$, and NaCl ranging from 0.1 to 1.0 M as indicated in each buffer's name: e.g., AnU-0.3 buffer contains 20 mM Tris-HCl, pH 7.4, 1 mM $MgCl_2$, and 0.3 M NaCl. All solutions were sterile-filtered prior to use, and the salt concentrations were confirmed by relative conductivity to a known standard. Radiolabeled [$\gamma$-$^{32}$P]ATP was obtained from New England Nuclear (Boston, MA).

*Proteins and Nucleic Acids.* Recombinant T4 uvsY protein was expressed and purified as previously described (*12*), and judged >98% pure by SDS−polyacrylamide gels stained with Coomassie Brilliant Blue. Purified protein was stored at −20 °C in uvsY storage buffer [20 mM Tris-HCl, pH 7.4, 100 mM NaCl, 0.2 mM EDTA, 1 mM DTT, 65% (w/v) glycerol] until needed, upon which it was exchanged into an appropriate AnU buffer by column chromatography over Sephadex G-25M (Pharmacia, Uppsala, Sweden) as per the manufacturer's instructions. Protein concentration was determined by the absorbance at 280 nm using a molar extinction coefficient of $\epsilon_{M,280nm} = 19\,180\ M^{-1}\ cm^{-1}$ as calculated (*21*) from the amino acid sequence (*22*). All uvsY protein stock solutions were nuclease-free as determined by sensitive agarose gel electrophoresis assays for degradation of ssDNA and dsDNA species (*23*).

Circular single-stranded DNA from bacteriophage M13mp19 was isolated by extraction from purified phage particles (*24*, *25*). The etheno-modified ($\epsilon$DNA) form of M13mp19 ssDNA was prepared as described previously (*26*). ssDNA and $\epsilon$DNA concentrations were determined by the phosphate−ash method as described (*12*, *27*). HPLC-purified oligonucleotide ($dT_{25}$) was purchased from Operon Technologies (Alameda, CA) and quantitated by the absorbance at 260 nm using the molar extinction coefficient of $\epsilon_{M,260nm} = 196\,912\ M^{-1}\ cm^{-1}$ provided by the manufacturer. Homo-oligonucleotide ($dT_{25}$) was 5′-end-labeled using T4 polynucleotide kinase (USB, Cleveland, OH) following previously established protocols (*28*).

*Analytical Ultracentrifugation Studies.* All analytical ultracentrifugation experiments reported in this paper were conducted either in a Beckman Optima XL-I or in a Beckman Optima XL-A analytical ultracentrifuge. Some preliminary experiments (data not shown) were conducted in a Beckman Model E. All three centrifuges were equipped with absorption optical systems, while the Optima XL-I was also equipped with Rayleigh interference optics. For experiments performed in the Optima XL-I, experimental data were collected using both optical systems in parallel whenever possible. Sedimentation velocity and equilibrium experiments were conducted between 20 and 25 °C under native (AnU buffers) or denaturing (6 M guanidine hydrochloride) conditions.

Sedimentation equilibrium experiments were performed in the Optima XL-I using the method of Yphantis (*29*). All experiments utilized a Beckman An50-Ti 8-hole rotor and cells equipped with either 2-sector or 6-sector charcoal-filled Epon centerpieces and sapphire windows. Initial loading concentrations for uvsY ranged from 0.05 to 0.2 mg/mL. Absorbance data were acquired at 280 nm as an average of 10 measurements at each radial position in 0.001 cm increments. The Rayleigh interference optical system on the XL-I uses a 675 nm laser diode light source, and direct video data capture. Video data were obtained at a resolution of 2048 × 96 pixels, corresponding to approximately 4.3 fringes. Equilibrium distributions were analyzed over a range of rotor speeds from 12 000 to 45 000 rpm, such that data were collected corresponding to a range of $\sigma = 2-7$, where

$$\sigma = M(1 - \bar{\nu}\rho)\omega^2/RT \qquad (1)$$

is the reduced apparent molecular weight (*29*). The state of equilibrium was evaluated by comparing successive scans taken 2 h apart and comparing each data set to the final scan. Equilibrium was achieved when rms deviations did not change significantly between the final three data sets, taken over a period of at least 8 h. Both absorbance and interference data were edited to remove extraneous data outside of the sample column. Data editing and evaluation of equilibria were performed using the programs REEDIT and MATCH, respectively, provided by the National Analytical Ultracentrifugation Facility at the University of Connecticut (Storrs, CT). Concentration profiles were then analyzed at the 95% confidence interval using the NONLIN curve-fitting package (*30*), allowing a global fit to $\sigma$. Conversion from the reduced apparent molecular weight ($\sigma$) was performed using molar mass and partial specific volume ($\bar{\nu}$) values calculated from the amino acid composition of uvsY (*22*), as described (*31*), equal to 15731.3 g/mol and 0.738 $cm^3/g$, respectively. This method results in $\bar{\nu}$ values that are typically within 1% of the measured $\bar{\nu}$ (*31*). It is important to note that errors in the calculation of $\bar{\nu}$ are magnified approximately 3-fold in the calculation of $M_r$ (*32*). Thus, the calculated mass reflects a 3% error introduced with the calculated $\bar{\nu}$. Solution densities ($\rho$) were calculated as described (*31*). SDS−polyacrylamide gel electrophoresis was performed on samples before and after each equilibrium experiment, and revealed no discernible degradation of the sample through the course of the experiment.

All sedimentation velocity experiments utilized 12 mm double sector charcoal- or aluminum-filled Epon centerpieces with either quartz (XL-A) or sapphire (XL-I) windows. Velocity experiments were conducted at rotor speeds between 26 000 and 50 000 rpm, using initial protein loading concentrations between 0.5 and 1.2 mg/mL. Sedimentation was monitored using absorbance and/or interference optics for protein samples, while the Rayleigh interferometer was used for protein−oligonucleotide complexes. Temperature and buffer conditions were as described above for equilibrium experiments. Data were interpreted using either the boundary analysis method of van Holde and Weischet (*33*) or the time derivative of the concentration profile, $g(s^*)$ (*34*). van Holde−Weischet analyses were performed using data collected from the Optima XL-A centrifuge, while all other analyses were performed using data collected from the Optima XL-I. All data used for $g(s^*)$ analyses were collected using the interference optics system of the Optima XL-I, using the smallest time interval possible (approximately 10 s between scans) and correcting for integral fringe shifts introduced during Fourier analysis. Sedimentation coefficients reported as $s_{20,w}$ have been corrected to standard conditions (20 °C in water), while $s^0_{20,w}$ values have additionally been corrected to reflect zero concentration of the sedimenting species. All sedimentation coefficients are reported in units of svedbergs (S), where 1 S = $1 \times 10^{-13}$ s. The relationship between $f$, the translational frictional coefficient, $M_b$, the buoyant molecular weight defined as $M(1 - \bar{\nu}\rho)$, and $s$ is given by the Svedberg equation (*35*), which is related to individual molecules by $N_0$, Avogadro's number:

$$s = M(1 - \bar{\nu}\rho)/N_0 f \qquad (2)$$

*Size Exclusion Chromatography.* Size exclusion HPLC of uvsY and uvsY−oligo($dT_{25}$) complexes was conducted between 20 and 25 °C in either AnU-0.3 or AnU-0.5 buffer using a 30 cm × 0.78 cm steel HPLC column containing TSK-GEL G2000$SW_{xl}$ (5 $\mu$m particle size, 125 Å pore size), which has a fractionation range of 5000−150 000 kDa for globular proteins. Alternatively, low-pressure size-exclusion chromatography of uvsY samples both alone and with $^{32}$P-labeled oligo($dT_{25}$) was conducted using a 19 cm × 0.7 cm glass column containing Sephacryl S-200HR (Pharmacia, Uppsala, Sweden), with a useful fractionation range for globular proteins of 5000−250 000 kDa. All chromatography experiments were performed in either AnU-0.3 or AnU-0.5 buffer. Columns were equilibrated over a minimum of 20 column volumes at a flow rate of 1.0 mL/min prior to sample addition. Void volume determination was performed using blue dextran, and each column was calibrated using a 14−158 kDa protein standard calibration kit (Pharmacia, Uppsala, Sweden). uvsY and/or oligonucleotide samples were exchanged into AnU-0.3 or AnU-0.5 and applied to the column. The flow rate was maintained at 1.0 mL/min for all separations. Column fractions were evaluated for protein and ssDNA content by absorbance at 214 nm (HPLC experiments) or 280 nm and liquid-scintillation counting (all other separations).

*ssDNA Binding Assays.* The ability of uvsY to bind ssDNA was evaluated by $\epsilon$DNA fluorescence enhancement as previously described (*12*). Fluorescence assays were performed at 25 °C in AnU buffers, using an SLM 8000 spectrofluorimeter. The excitation and emission wavelengths were 300 and 405 nm, respectively.

Table 1: Summary of Sedimentation Velocity Results for uvsY

| species | solvent[a] | $s^0_{20,w}$[b] |
|---|---|---|
| uvsY | <170 mM NaCl | >10 |
| | 180−200 mM NaCl | 6−19 |
| | >200 mM NaCl | 6.0 |
| oligo($dT_{25}$) | 300 mM NaCl | <2.0 |
| | 500 mM NaCl | <2.0 |
| uvsY + oligo($dT_{25}$) | 300 mM NaCl | 6.5[c] |
| | 500 mM NaCl | 6.0[c] |

[a] AnU buffer (20 mM Tris, pH 7.4, 1.0 mM $MgCl_2$) with [NaCl] as indicated. [b] The sedimentation coefficient corrected to zero concentration and 20 °C in water. See text for centrifugation conditions. [c] For these experiments, Rayleigh interferometry was used to observe sedimentation. Under these conditions, the Rayleigh optical system is not sufficiently sensitive to detect oligo($dT_{25}$). See text for details.

## RESULTS

*Self-Association of uvsY Protein.* Sedimentation velocity of the uvsY protein under varying conditions of salt ([NaCl] = 100−500 mM in AnU buffer) reveals a highly salt-dependent behavior consistent with self-association. A marked transition in uvsY sedimentation properties occurs at a salt concentration of approximately 200 mM NaCl, as shown in Figures 1 and 2, and summarized in Table 1. Under high-salt conditions (>200 mM NaCl in AnU buffer), sedimenting boundaries remain highly symmetrical throughout the experiment. Typical of this behavior is the experiment represented in Figure 1A,B, performed at 450 mM NaCl in AnU buffer. The van Holde−Weischet plot of these data (Figure 1B) shows convergence to a single value of $s_{20,w} = 6.2$ ($s^0_{20,w} = 6.0$), indicating a monodisperse population of sedimenting species displaying little concentration dependence over the concentration range of the boundary. uvsY protein exhibits essentially identical sedimentation behavior at salt concentrations as high as 1 M NaCl in AnU buffer (data not shown), the highest salt concentration tested, demonstrating that the $s^0_{20,w} = 6.0$ species of uvsY represents a highly salt-stable form of this protein. We observe no forms of uvsY protein sedimenting slower than 6S under any native (AnU) buffer conditions. Since the sequence-derived mass of uvsY protein is only 15.8 kDa, it is likely that this "stable" 6S form of uvsY is a multimer. We demonstrate in a later section that the 6S species in fact corresponds to a hexamer of uvsY protein.

The 6S form of uvsY protein predominates at NaCl concentrations as low as 200 mM; however, the concentration dependence of $s$ becomes more pronounced with decreasing salt. This behavior is typified by the data in Figure 1C,D, representing velocity runs performed at 230 mM NaCl in AnU buffer. The sedimenting boundary remains highly symmetrical (Figure 1C), and van Holde−Wesichet analysis reveals convergence to $s_{20,w} = 6.2$, but with slight increases of $s$ in the most concentrated fractions consistent with concentration-dependent association into larger aggregated forms of uvsY protein (Figure 1D; see also Figure 2). In contrast to the high-salt experiments, velocity runs performed at salt concentrations below 200 mM NaCl reveal dramatically faster sedimenting forms of uvsY protein, indicating a more heterogeneous population of aggregate size. Repre-

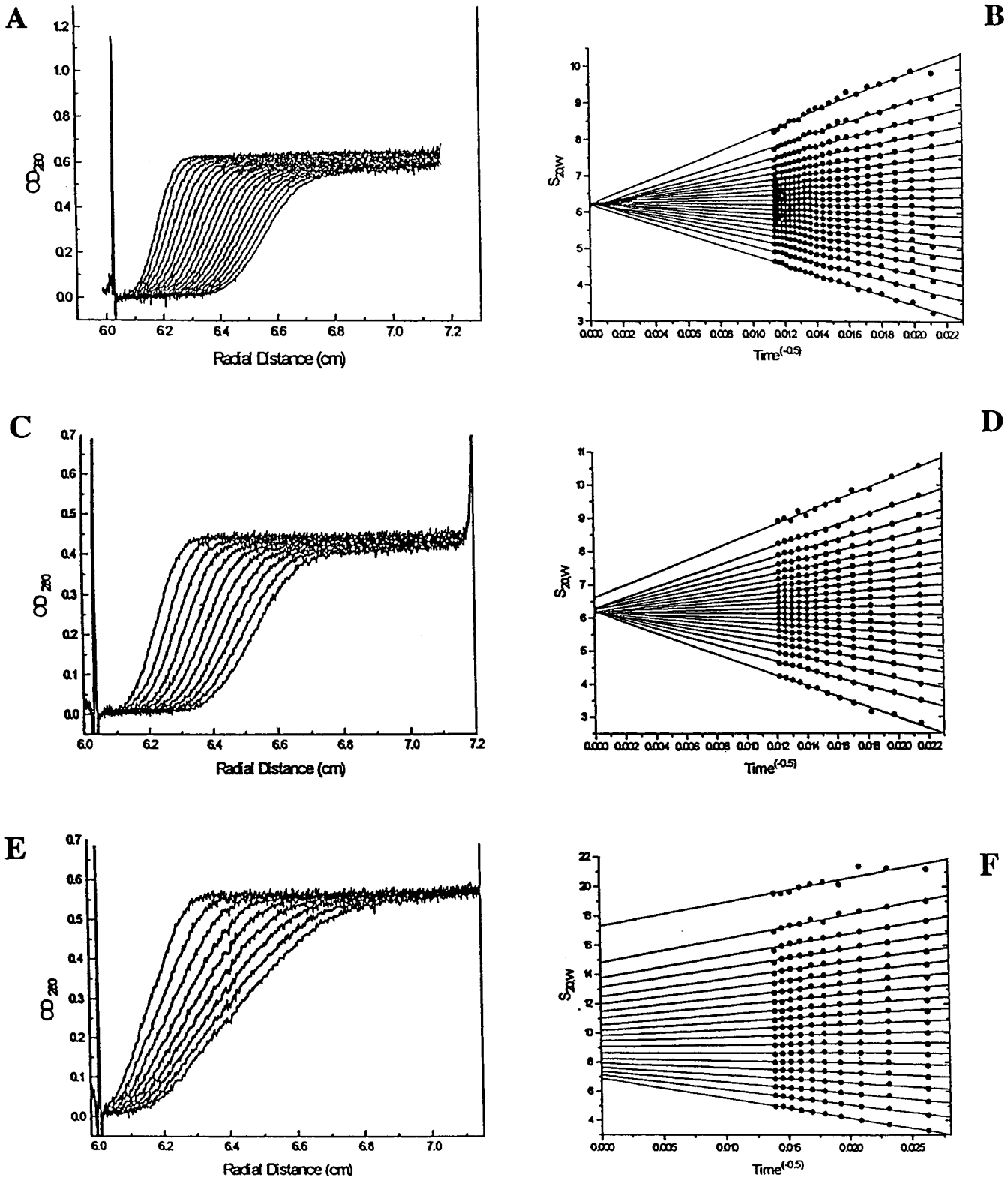


FIGURE 1: Sedimentation velocity of uvsY. Sedimentation velocity of uvsY at an initial loading concentration of 0.5 mg/mL was observed using the absorbance optical system of the XL-A in AnU buffer plus 450 mM NaCl (A), 230 mM NaCl (C), and 180 mM NaCl (E). Rotor speeds were 42 000 rpm (A, C) and 35 000 rpm (E), respectively. Corresponding van Holde−Weischet analyses for these data are presented using 95% of the sedimenting boundary (B, D, F, respectively). See text for details.

sentative of this behavior is the experiment shown in Figure 1E,F, performed at 180 mM NaCl in AnU buffer. Here, the sedimenting boundary develops a highly asymmetrical shape over the period of sedimentation (Figure 1E), indicating a mixed population of species. The corresponding van Holde−Weischet plot (Figure 1F) shows no convergence to a single *s* value, but instead a highly concentration-dependent system with $s_{20,w}$ ranging from approximately 6.5 to 18 (see also Figure 2).

To further evaluate the salt-dependent association of uvsY protein, sedimentation velocity experiments were conducted over NaCl concentrations from 110 mM to 250 mM in AnU

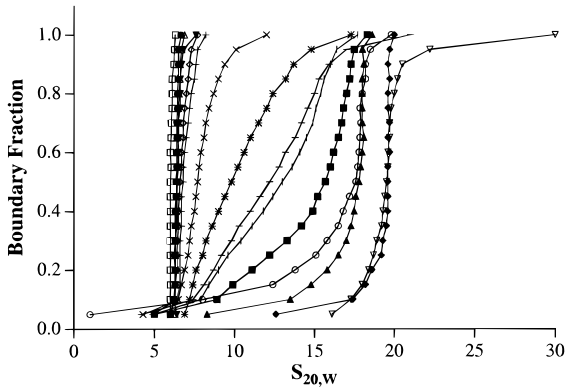


FIGURE 2: Integral distribution of uvsY as a function of salt. Curves represent the distribution of *s* for uvsY under conditions of varying NaCl concentration: 110 mM (◆), 120 mM (▽), 130 mM (▲), 140 mM (○), 150 mM (■), 160 mM (|), 170 mM (−), 180 mM (*), 190 mM (×), 200 mM (+), 210 mM (◇), 220 mM (▼), 230 mM (△), 240 mM (●), 250 mM (□). Integral distribution plots were generated from sedimenting boundaries of uvsY at 0.5 mg/mL using 95% of the boundary. Markers are connected for clarity.

buffer, in 10 mM increments of NaCl. The boundary fractions displayed in van Holde−Weischet plots such as those shown in Figure 1 were plotted against extrapolated $s_{20,w}$ values to yield the integral distributions of sedimenting species (Figure 2), giving an indication of the concentration dependence and overall heterodispersity of the system at each salt concentration. As shown in Figure 2, NaCl concentrations of 200 mM or greater give rise to largely salt- and concentration-independent sedimentation behavior of uvsY protein, as indicated by the nearly overlaying vertical lines in the integral distribution plots. All of these data are consistent with a single uvsY species of $s_{20,w} = 6.2$ existing in AnU-0.2 buffer and at higher [NaCl], though with some tendency toward further concentration-dependent association at the lower end of this salt range. In contrast, the integral distributions for experiments performed in 110−190 mM NaCl (Figure 2) are much more complicated, showing extreme sensitivities to both salt and protein concentrations consistent with the results obtained at 180 mM NaCl and shown in Figure 1E,F. In some cases, small changes in salt concentration resulted in relatively large redistribution of the average *s* value (see 150 and 160 mM NaCl data in Figure 2). At the lowest salt concentration shown (110 mM), the distribution appears to converge again on a single species of $s_{20,w} = 19$, although concentration dependence is still evident (Figure 2).

A simple model to explain the data shown in Figures 1 and 2 is that the "high-salt" ($s^0_{20,w} = 6.0$) species of uvsY represents a stable oligomeric structure of this protein, and that this 6S species weakly self-associates under low-salt conditions into more highly aggregated forms. This model is supported by the following observations (data not shown): First, a uvsY sample in 180 mM NaCl was subjected to velocity sedimentation and exhibited the characteristic heterogeneous sedimentation behavior like that shown in Figure 1E,F. After the initial run, this sample was "spiked" with NaCl to a final concentration of 350 mM without removing the sample from the cell. The sample was centrifuged again, and this time displayed monodisperse sedimentation behavior with $s_{20,w} = 6.2$, essentially identical to the "high-salt" samples shown in Figure 1A−D. Second, samples run under high-salt conditions and displaying monodisperse 6S behavior, recovered and exchanged into low-salt buffers such as AnU-0.18, exhibit heterogeneous sedimentation behavior with $s_{20,w} = 6.5-19$. These two observations (not shown) suggest that the 6S form of uvsY protein is capable of fully reversible association into faster sedimenting forms in a salt-dependent manner.

Table 2: Summary of Sedimentation Equilibrium Results for uvsY[a]

| solvent[b] | solvent density[c] | $M_{app}$ (kDa)[d] | $K_a$[e] |
|---|---|---|---|
| 290 mM NaCl | 1.011 | 95.0 ± 1.2 | $1.5 \times 10^6$ $M^{-1}$ |
| 300 mM NaCl | 1.011 | 97.2 ± 4.8 | ND |
| 500 mM NaCl | 1.019 | 98.6 ± 3.9 | ND |
| 6.0 M Gua-HCl | 1.142 | 18.4 ± 1.9 | ND |

[a] Results summarized from data collected by both interference and absorbance optics over multiple rotor speeds and protein loading concentrations. [b] AnU buffer (20 mM Tris, pH 7.4, 1.0 mM $MgCl_2$) with [NaCl] as indicated. [c] Densities as calculated from the method of Laue et al. (1992) and reported at 20 °C. [d] Apparent mass calculated from the reduced molecular weight as described under Experimental Procedures. Error represents the 95% confidence interval. [e] Molar association constants defined for hexamer ↔ dodecamer equilibrium. Solvents containing NaCl concentrations of 300 mM and above were not adequately described by an associating model, and were therefore not determined.

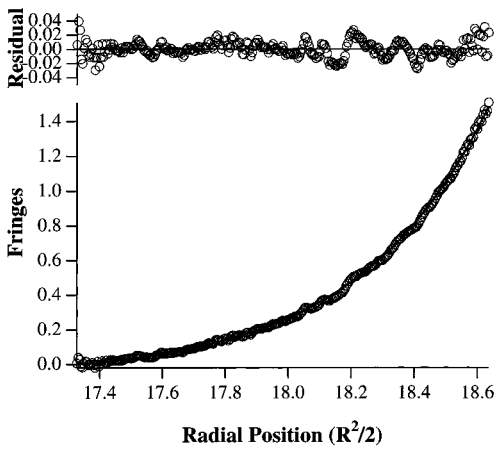


FIGURE 3: Sedimentation equilibrium of uvsY in AnU plus 500 mM NaCl. Data were collected after 27 h at 15 000 rpm, 22 °C, using the Rayleigh interferometer of the XL-I. Here, the initial loading concentration of uvsY was 0.07 mg/mL, and the reduced molecular weight ($\sigma$) is approximately 2.4, corresponding to a homodisperse solute of $M = 97.4 \pm 1.4$ kDa. These data and others were used in global fitting to obtain the results given in Table 2.

*Stoichiometry of the 6S uvsY Species.* The stoichiometries of the 6S and higher forms of uvsY protein were assessed using equilibrium sedimentation. Multiple sedimentation equilibrium gradients were globally fit to obtain the reduced apparent molecular weight, $\sigma$, over a range of protein concentrations and rotor speeds. Results are summarized in Table 2. At 300 mM NaCl, conditions in which uvsY sediments exclusively as a 6S species in velocity experiments, multiple equilibrium data sets are best described by a model invoking a single ideal species of $M_{app} = 97$ kDa (Figure 3), which is within 3% of the predicted mass of a 95 kDa hexamer of uvsY protein. Thus, we conclude that the 6S form of uvsY is composed of six 15.8 kDa monomers ($uvsY_6$) which form the most stable quaternary structure of the uvsY protein. There was no significant change in the apparent mass of uvsY observed over an NaCl range from 300 to 1000 mM (data not shown), indicating that the

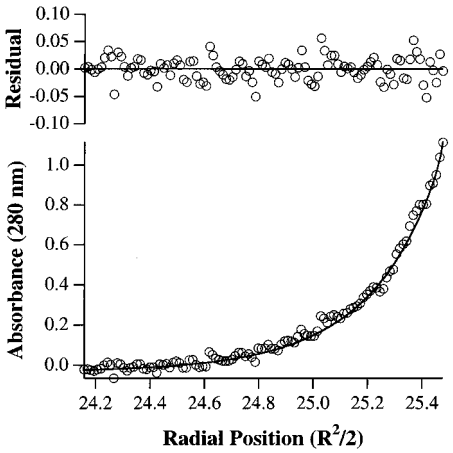


FIGURE 4: Sedimentation equilibrium of uvsY in AnU plus 290 mM NaCl. Multiple data sets fit over a range of rotor speeds from 15 000 to 25 000 rpm indicate a hexamer−dodecamer equilibrium with a $K_a$ of approximately $1.5 \times 10^6$ $M^{-1}$. This representative data set was obtained at 18 000 rpm using the absorbance optical system of the XL-I and an initial loading concentration of 0.09 mg/mL uvsY.

hexamer remains stable throughout this salt range and does not dissociate into smaller components. Sedimentation equilibrium experiments conducted at lower salt concentrations ([NaCl] < 300 mM) could not be adequately fit with a single species model. Sedimentation equilibrium data at [NaCl] between 250 and 300 mM were best described by a model in which uvsY hexamers ($uvsY_6$) weakly associate into oligomeric forms of $(uvsY_6)_n$ where $n = 2$, 3, or 4. An association constant of $1.5 \times 10^6$ $M^{-1}$ was estimated for the presumed $uvsY_6 \leftrightarrow (uvsY_6)_2$ equilibrium in 290 mM NaCl (Figure 4). The behavior of uvsY in salt concentrations below 200 mM NaCl could not be interpreted by equilibrium sedimentation. A slow loss of protein was observed during the approach to equilibrium, most likely due to the development of very large aggregates that were removed from the solution column by sedimentation. Equilibrium experiments were also conducted in 6.0 M guanidine hydrochloride (data not shown; results summarized in Table 2), conditions in which most proteins are fully denatured. These data were best described by a single species of $M_{app} = 18.4 \pm 1.9$ kDa, approximating the molecular mass of the uvsY monomer.

uvsY samples recovered after equilibrium sedimentation runs were evaluated for both protein degradation and ssDNA-binding activity (data not shown). SDS−polyacrylamide gel electrophoresis revealed no detectable proteolytic degradation of uvsY protein in any sample over the course of equilibrium runs. In addition, all native samples (excluding those treated with Gua-HCl) retained the ability to bind to and enhance the fluorescence of etheno-modified M13mp19 ssDNA ($\epsilon$DNA) within normal parameters established by Sweezy and Morrical (*12*).

*Binding of ssDNA by the uvsY Hexamer.* Previous characterization of the ssDNA binding activity of uvsY (*12*) revealed that this protein binds tightly to single-stranded polynucleotides throughout the salt range of 0−400 mM NaCl in AnU buffer. Salt concentrations at which uvsY exists exclusively as the 6S hexamer fall well within this range, suggesting that uvsY hexamers should be competent to bind to ssDNA. To test the ssDNA binding activity of uvsY hexamers, the homo-oligonucleotide $dT_{25}$ (MW = 7519) was added in stoichiometric amounts (1:1 molar ratio of oligo:hexamers), and the resulting mixtures were analyzed by sedimentation velocity analyses. The 25-mer length was chosen since it is close to the minimum binding site size predicted for a uvsY hexamer assuming a binding site size of 4 nucleotides per uvsY *monomer* (*12*). Separate experiments (data not shown) employing $\epsilon$DNA competition binding assays established that oligo($dT_{25}$) binds tightly to uvsY in 300 mM NaCl but weakly or not at all in 500 mM NaCl (both in AnU buffer). We expected that if ssDNA binding required the dissociation of the hexamer, then either free or oligo-bound subhexameric forms would be evident, appearing as slowly sedimenting species. Conversely, if no dissociation occurred, the free vs ssDNA-bound hexamer should be apparent, with a corresponding change in sedimentation properties upon ssDNA binding. Conditions were selected such that the concentrations of oligonucleotide used were essentially undetectable by the Rayleigh interferometer. Therefore, only the sedimentation of the protein component is directly observed.

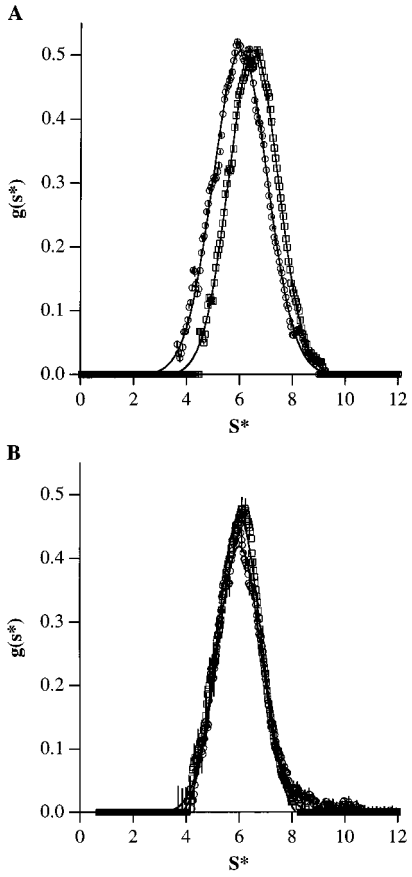


FIGURE 5: Time derivative of the concentration profile for uvsY and uvsY−oligo($dT_{25}$). (A) Binding of oligo($dT_{25}$) by uvsY in 300 mM NaCl is indicated by a 0.5S change in the sedimentation coefficient of the complex (□) over that of uvsY alone (○). (B) Conversely, the addition of oligo($dT_{25}$) (□) had no effect on the sedimentation behavior of uvsY (○) in 500 mM NaCl, indicating that this salt concentration was sufficient to prevent uvsY−oligo($dT_{25}$) complex formation. Error bars indicate the standard error of the mean. See text for details.

Analysis of the time derivative of the sedimenting boundary, $g(s^*)$, revealed that in the absence of oligo($dT_{25}$), uvsY sediments homogeneously as the expected $s^0_{20,w} = 6.0$ species in both 300 and 500 mM NaCl in AnU buffer (Figure 5). In the presence of oligo($dT_{25}$) in 300 mM NaCl, the measured

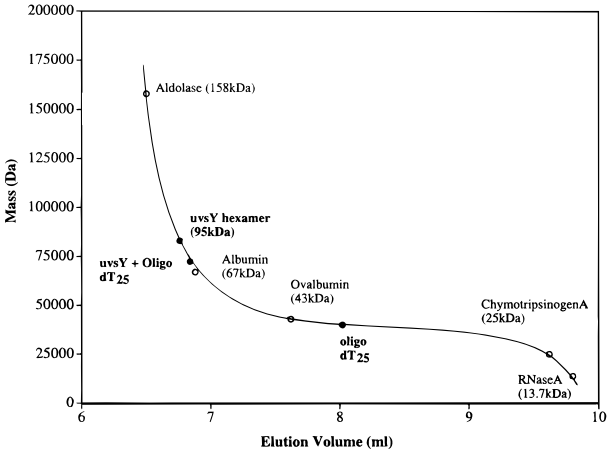


FIGURE 6: HPLC gel filtration of uvsY, oligo($dT_{25}$), and the bound complex. Upon oligo($dT_{25}$) binding, the uvsY−ssDNA complex is further retained by the matrix. The elution positions of uvsY−ssDNA, uvsY, and oligo($dT_{25}$) are indicated (●) relative to known standards (○) as shown.

$s^0_{20,w}$ value was 6.5, representing a reproducible and statistically significant increase of 0.5S over uvsY alone (Figure 5A). Although a slight increase in *s* upon oligo binding would be expected if the overall shape of the oligo−uvsY complex remained similar to that of uvsY alone, the 0.5S increase observed here was somewhat larger than anticipated given the relationship of both *f* and $M_b$ to *s* (eq 2). The *g*(*s**) plot for uvsY + oligo at 300 mM NaCl (Figure 5A) revealed no peaks or shoulders at higher or lower *s* values, and the peak observed remained highly symmetrical with a width approximately equal to the peak widths observed for uvsY alone at 300 and 500 mM NaCl (Figure 5). The simplest interpretation of these results is that the uvsY hexamer binds to oligo($dT_{25}$) as an intact unit, forming a discrete $uvsY_6$−($dT_{25}$) species of $s^0_{20,w} = 6.5$ under the tight uvsY−oligo binding conditions observed in AnU-0.3 buffer. The significant increase in the observed sedimentation behavior of the complex might reflect a conformational change in the uvsY hexamer upon ssDNA binding (see below). In contrast, at 500 mM NaCl, where uvsY−oligo interactions are weak or nonexistent, no change in either the *s* value or the shape of the *g*(*s**) profile is seen between samples containing or lacking oligo($dT_{25}$) (Figure 5B). Thus, the oligo-dependent increase in $s^0_{20,w}$ value from 6.0 to 6.5 is seen only under salt conditions permissive for uvsY−($dT_{25}$) interactions as determined independently by fluorometric ϵDNA competition (*12*).

The interaction of uvsY with oligo($dT_{25}$) was also examined by size exclusion chromatography. Here, a 5′-$^{32}$P-labeled oligo($dT_{25}$) species was preincubated with uvsY in AnU-0.3 buffer and applied to a low-pressure sizing column equilibrated in the same buffer. The radiolabeled oligo appears to coelute exclusively with uvsY hexamers (data not shown), supporting the notion that the uvsY hexamer binds to oligo($dT_{25}$) as an intact unit. Curiously, separation of the oligo-bound hexamer from the free, uncomplexed hexamer by size-exclusion HPLC shows a retention time for the oligo−uvsY complex that is unexpectedly longer than the free hexamer (Figure 6). By HPLC, the apparent mass of the uvsY−oligo complex is approximately 70 kDa as compared with known calibration standards, significantly smaller than the calculated mass (102 kDa) of a $uvsY_6$−($dT_{25}$) complex. The uvsY protein alone elutes as a single 90 kDa species, consistent with the calculated 95 kDa mass of a uvsY hexamer, while the oligo($dT_{25}$) molecule alone elutes in much later fractions (Figure 6). Thus, the oligo-bound form of uvsY is retained on the HPLC column as a molecule of much smaller hydrodynamic radius than the uvsY hexamer alone. Both the HPLC and the sedimentation data can be explained if oligo($dT_{25}$) binding by the uvsY hexamer results in significant compaction of the overall structure. This and other possibilities are discussed in greater detail below.

## DISCUSSION

Hydrodynamic studies of the bacteriophage T4 uvsY protein have revealed the following: (1) that uvsY protein exists as a stable hexamer in solution under conditions of moderate to high salt concentrations; (2) that uvsY hexamers undergo further, reversible self-association to higher forms in a salt- and concentration-dependent manner; and (3) that the uvsY hexamer binds to ssDNA as an intact unit, possibly resulting in significant conformational changes upon binding. These results constitute the first physical characterization of the oligomeric structure of the uvsY protein.

Our observation that uvsY exists in hexameric and higher forms in solution and when bound to ssDNA helps to resolve an apparent inconsistency in the previous uvsY literature: Kodadek and co-workers reported that uvsY protein may be chemically cross-linked to itself in solution and when bound to ssDNA, under conditions required for uvsX−ssDNA filament assembly and DNA strand exchange (*15*, *20*). Treated samples subjected to SDS−PAGE revealed cross-linked dimers of uvsY protein. Nevertheless, Sweezy and Morrical (*12*) demonstrated that uvsY protein binds noncooperatively to ssDNA. Our observation that uvsY binds to ssDNA as a hexamer explains why cross-linking occurs even with uvsY protein which is noncooperatively bound to ssDNA. At the same time, the chemical trapping of uvsY dimers is consistent with a hexameric quaternary structure for uvsY protein, given that many protein hexamers appear to be organized as trimers-of-dimers (*36*). The combined data render it highly probable that uvsY functions either in hexameric or in some related oligomeric form during presynapsis and DNA strand exchange reactions, at least in vitro.

But what about in vivo? The monodisperse sedimentation pattern of uvsY observed at moderate to high salt concentrations indicates that uvsY hexamers are very stable in the salt concentrations tested. In the integral distribution plots shown in Figure 2, no dissociation of the 6S hexamers is evident even in the least concentrated fractions of the boundaries (see data for [NaCl] ≥200 mM in Figure 2). Therefore, the $K_d$ for hexamer dissociation must be in the sub-micromolar range given the uvsY concentrations (20−50 μM) at which the velocity runs were performed. This suggests that the uvsY protein exists as a hexamer (or larger aggregate) within the T4-infected *E. coli* cell, since the in vivo concentration of uvsY is estimated to be on the order of micromolar quantities during its period of active expression from middle to late infection (*37*). Thus, uvsY protein would appear to participate in general recombination events in vivo in oligomeric form.

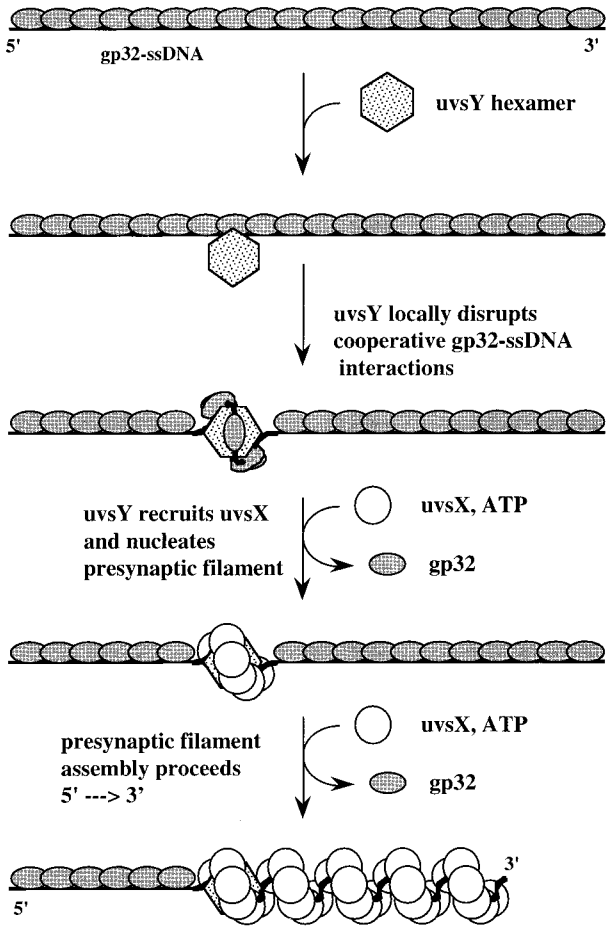


FIGURE 7: Model for nucleation of the T4 presynaptic filament by the uvsY protein. Here, oligomeric uvsY is able to bind the gp32−ssDNA complex, inducing a conformational change in the filament, gp32 protein, or both. The resulting structure may then act as a target site for the uvsX recombinase, which polymerizes 5′ → 3′, displacing the gene 32 protein from the strand.

The issue of ssDNA conformation within the uvsY−ssDNA complex is emerging as one of central importance to the T4 recombination problem. The existence of a stable hexameric form of uvsY protein capable of interacting with ssDNA could therefore have important implications for the mechanism of uvsY action. A key question is whether ssDNA interacts with multiple subunits of the uvsY hexamer. Multiple interactions within the uvsY complex could lead to wrapping of the ssDNA around the hexamer. In addition to wrapping, the observed change in hydrodynamic properties of the hexamer might reflect a conformational change of the uvsY hexamer upon ssDNA binding, consistent with overall compaction of the complex upon ssDNA association. Conceivably, wrapping or other structural distortions caused by $uvsY_6$−ssDNA interactions could play a role in nucleating uvsX−ssDNA filament formation and/or in destabilizing gp32−ssDNA complexes for displacement by uvsX. Such a scheme is depicted in the hypothetical model shown in Figure 7. Here, the uvsY hexamer is able to bind the gp32−ssDNA complex. Binding of the gp32−ssDNA induces a conformational change in the uvsY−ssDNA filament, gp32 protein, or both, that results in lower affinity of the gp32 protein for ssDNA. The structure formed upon uvsY binding is recognized by the uvsX recombinase which nucleates at the uvsY−ssDNA structure and displaces gp32 from the nucleoprotein filament. Experiments in progress should help to resolve whether ssDNA binds to multiple subunits of uvsY hexamers, and whether $uvsY_6$−ssDNA complex formation involves wrapping of the ssDNA.

A fascinating correlation exists between the hydrodynamic behavior of uvsY protein and its ssDNA-binding activity. Sweezy and Morrical (*12*) studied the enhancement of $\epsilon$DNA fluorescence caused by uvsY binding, and found that the maximum extent of fluorescence enhancement is affected strongly by salt concentration. Above a threshold salt concentration of approximately 200 mM NaCl in AnU buffer (or 200 mM KOAc in equivalent buffer), uvsY binding enhances $\epsilon$DNA fluorescence by 2−2.5-fold at saturation, similar to results obtained with many other ssDNA-binding proteins including the T4 gp32 and gp59 proteins, the *E. coli* recA protein, and the yeast RP-A protein (*18*, *38*, *39*, *26*, *40*). However, at NaCl concentrations below 200 mM, uvsY binding induces greater enhancements of $\epsilon$DNA fluorescence at saturation, as high as 6-fold in some experiments (*12*). The expected 2−2.5-fold fluorescence enhancement seen with the proteins mentioned above and with uvsY protein at [NaCl] >200 mM has been ascribed to the extension of the polynucleotide backbone and to the unstacking of bases in $\epsilon$DNA. The hyperenhancement of $\epsilon$DNA fluorescence seen with uvsY at low salt suggests that other enhancement mechanisms, perhaps representing multiple conformations of the uvsY−$\epsilon$DNA complex, may be at work as well. Most intriguing is that the transition from normal to hyperenhancement of $\epsilon$DNA fluorescence and the transition from hexameric to larger forms of uvsY in solution occur at the same salt concentration: 200 mM NaCl. One possibility is that the different fluorescent states of uvsY−$\epsilon$DNA represent changes in the oligomeric structure of uvsY bound to $\epsilon$DNA and/or differences in the degree to which the polynucleotide is wrapped around uvsY oligomers.

The uvsY protein plays a key role in assembling the presynaptic filaments required for general recombination in bacteriophage T4. Analogous roles have been proposed for accessory proteins in other recombination systems, including the recF/OR proteins of *E. coli*, and the Rad52 and Rad55/57 proteins in *S. cerevisiae* (*41*−*46*). Through continued physical and biochemical studies of uvsY protein, we hope to develop a rigorous model of uvsY structure and function, one which will hopefully shed light on recombination mechanisms used by many organisms.

## ACKNOWLEDGMENT

We gratefully acknowledge Drs. Jeff Hansen, Boris Demmeler, and Cindy Turgeon (University of Texas Health Science Center at San Antonio) for performing sedimentation velocity runs on the Beckman Optima XL-A instrument and for conducting van Holde−Weischet analyses of velocity data. We also gratefully acknowledge Dr. Kenneth Mann (University of Vermont) for training and assistance in operating the Beckman Model E instrument, Dr. Thomas Laue (University of New Hampshire) for discussion, advice, and encouragement, and Mark Sweezy of this laboratory for assistance with $\epsilon$DNA fluorescence enhancement assays.

## REFERENCES

1. Yonesaki, T., and Minagawa, T. (1989) *J. Biol. Chem. 264*, 7814.

2. Kodadek, T., Gan, D.-C., and Stemke-Hale, K. (1989) *J. Biol. Chem. 264*, 16451.
3. Harris, L. D., and Griffith, J. D. (1989) *J. Mol. Biol. 206*, 19.
4. Morrical, S. W., and Alberts, B. M. (1990) *J. Biol. Chem. 265*, 15096.
5. Formosa, T., and Alberts, B. M. (1986) *J. Biol. Chem. 261*, 6107.
6. Morrical, S. W., Wong, M. L., and Alberts, B. M. (1991) *J. Biol. Chem. 266*, 14031.
7. Cunningham, R. P., and Berger, H. (1977) *Virology 80*, 67.
8. Melamede, R. J., and Wallace, S. S. (1977) *J. Virol. 24*, 28.
9. Melamede, R. J., and Wallace, S. S. (1978) *FEBS Lett. 87*, 12.
10. Melamede, R. J., and Wallace, S. S. (1980) *Mol. Gen. Genet. 177*, 501.
11. Kreuzer, K. N., and Morrical, S. W. (1994) in *Molecular Biology of Bacteriophage T4* (Karam, J. D., Ed.) p 28, American Society for Microbiology, Washington, DC.
12. Sweezy, M. A., and Morrical, S. W. (1997) *J. Mol. Biol. 266*, 927.
13. Formosa, T., and Alberts, B. M. (1984) *Cold Spring Harbor Symp. Quant. Biol. 49*, 363.
14. Hurley, J. M., Chervitz, S. A., Jarvis, T. C., Singer, B. S., and Gold, L. (1993) *J. Mol. Biol. 229*, 398.
15. Jiang, H., Giedroc, D., and Kodadek, T. (1993) *J. Biol. Chem. 268*, 7904.
16. Yassa, D. S., Chou, K.-M., and Morrical, S. W. (1997) *Biochimie 79*, 275.
17. Griffith, J., and Formosa, T. (1985) *J. Biol. Chem. 260*, 4484.
18. Kowalczykowski, S. C., Lonberg, N., Newport, J. W., and von Hippel, P. H. (1981) *J. Mol. Biol. 145*, 75.
19. Newport, J. W., Lonberg, N., Kowalczykowski, S. C., and von Hippel, P. H. (1981) *J. Mol. Biol. 145*, 105.
20. Jiang, H., Salinas, F., and Kodadek, T. (1997) *Biochem. Biophys. Res. Commun. 231*, 600.
21. Gill, S. C., and von Hippel, P. H. (1989) *Anal. Biochem. 182*, 319.
22. Gruidl, M. E., and Mosig, G. (1986) *Genetics 114*, 1061.
23. Morrical, S. W., Hempstead, K., and Morrical, M. D. (1994) *J. Biol. Chem. 269*, 33069.
24. Yamamoto, K. R., Alberts, B. M., Benzinger, R., Lawhorne, L., and Trieber, G. (1970) *Virology 40*, 734.
25. Miller, H. (1987) *Methods Enzymol. 152*, 145.
26. Menetski, J. P., and Kowalczykowski, S. C. (1985) *J. Mol. Biol. 181*, 281.
27. Ames, B. N. (1966) *Methods Enzymol. 8*, 115.
28. Sambrook, J., Fritsch, E. F., and Maniatis, T. (1989) in *Molecular Cloning, a Laboratory Manual*, 2nd ed., Cold Spring Harbor Laboratory Press, Cold Spring Harbor, NY.
29. Yphantis, D. A. (1964) *Biochemistry 3*, 297.
30. Johnson, M. L., Correia, J. C., Yphantis, D. A., and Halvorson, H. R. (1981) *Biophys. J. 36*, 575.
31. Laue, T. M., Shah, B. D., Ridgeway, T. M., and Pelletier, S. L. (1992) in *Analytical Ultracentrifugation in Biochemistry and Polymer Science* (Harding, S. E., Rowe, A. J., and Horton, J. C., Eds.) p 90, Royal Society of Chemistry, Cambridge, U.K.
32. Schachman, H. K (1957) *Methods Enzymol. 4*, 32.
33. van Holde, K. E., and Weischet, W. O. (1978) *Biopolymers 17*, 1387.
34. Stafford, W. F. (1992) *Anal. Biochem. 203*, 295.
35. Svedberg, T. (1940) in *The Ultracentrifuge* (Svedberg, T., and Pederson, K. O., Eds.) Johnson Reprint Corp., New York.
36. Dong, F., Gogol, E. P., and von Hippel, P. H. (1995) *J. Biol. Chem. 270*, 97403.
37. Cowan, J., D'Acci, K., Guttman, B., and Kutter, E. (1994) in *Molecular Biology of Bacteriophage T4* (Karam, J. D., Ed.) p 520, American Society for Microbiology, Washington, DC.
38. Lefebvre, S. D., and Morrical, S. W. (1997) *J. Mol. Biol. 272*, 312.
39. Silver, M. S., and Fersht, A. R. (1982) *Biochemistry 21*, 6066.
40. Alani, E., Thresher, R., Griffith, J. D., and Kolodner, R. D. (1992) *J. Mol. Biol. 227*, 54.
41. Umezu, K., Chi, N. W., and Kolodner, R. D. (1993) *Proc. Natl. Acad. Sci. U.S.A. 90*, 3875.
42. Umezu, K., and Kolodner, R. D. (1994) *J. Biol. Chem. 269*, 30005.
43. Shan, Q., Bork, J. M., Webb, B. L., Inman, R. B., and Cox, M. M. (1997) *J. Mol. Biol. 265*, 519.
44. Firmenich, A. A., Elias-Arnanz, M., and Berg, P. (1995) *Mol. Cell Biol. 15*, 1620.
45. Sung, P. (1997) *Genes Dev. 11*, 1111.
46. Sung, P. (1997) *J. Biol. Chem. 272*, 28194.

BI9800956